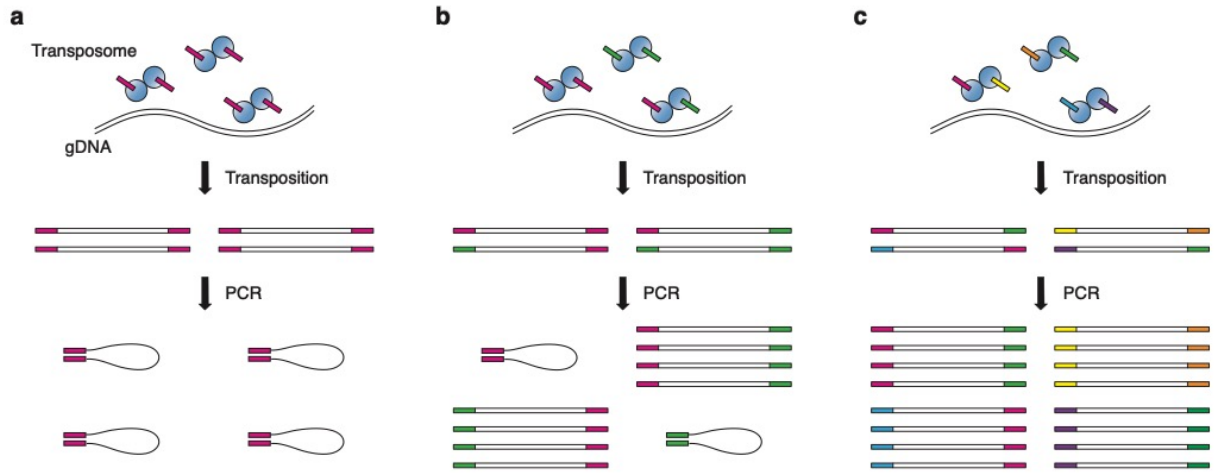

SI Appendix Figure S1

Tags introduced by Tn5 transposition function as PCR primers for amplification of the transposed fragments. The chance to for a fragment to be tagged by the same sequence is inversely proportional to the number of transposon tags. With only one tag (**A**), PCR templates tend to form hairpin loop structures that could block the annealing of primers. For Illumina Nextera kit (**B**), two different tags are randomly inserted and hence 50% of DNA templates would be lost. With N different tags in META (**C**), the chance to have a DNA fragment form the hairpin loop structure is 1/N.

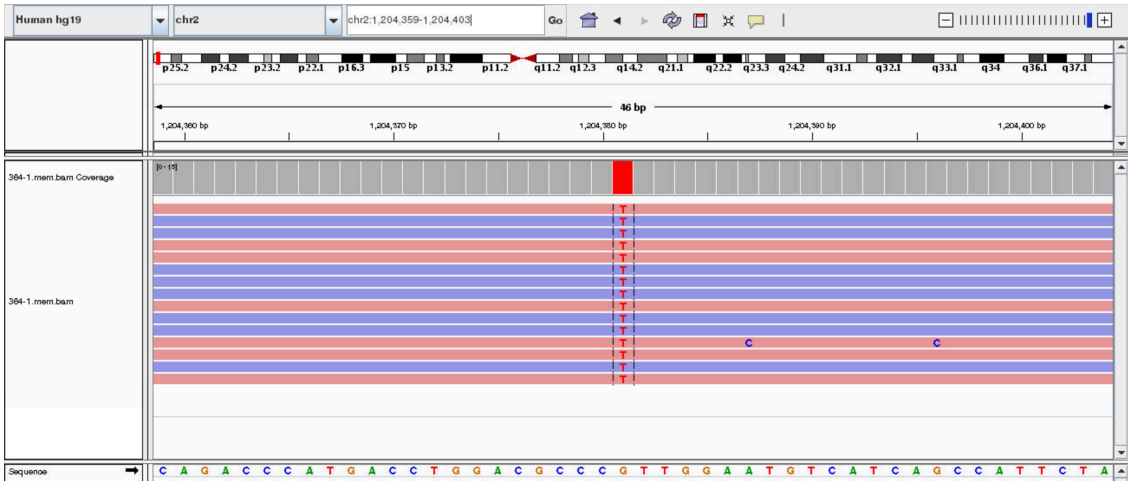

SI Appendix Figure S2

Example of a de novo mutation (G>T) detected by META-CS viewed in Integrative Genomics Viewer (IGV). Reads from two complementary strands are shown in red and blue. The mutated base was detected in both strands of the DNA.

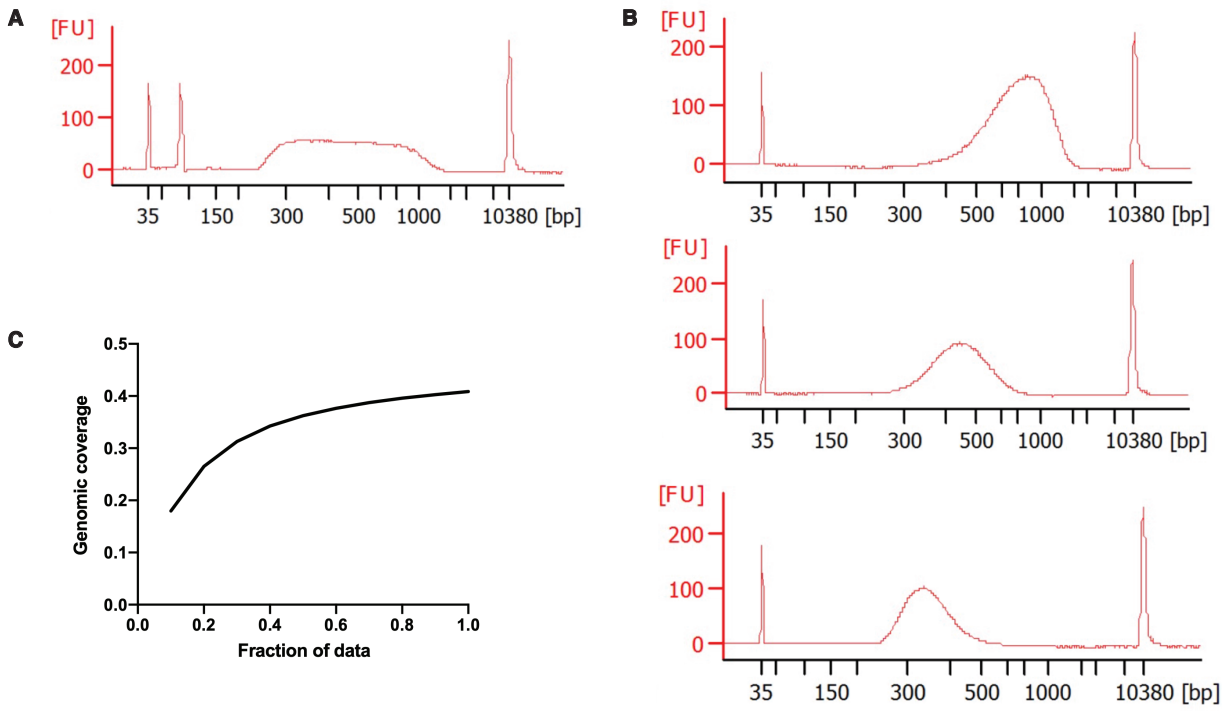

SI Appendix Figure S3

Fragment length distributions after whole-genome amplification and sequencing saturation curve. (**A**) Bioanalyzer trace of a representative cell after META-CS amplification. FU: fluorescence units. (**B**) Bioanalyzer trace of pooled single-cell libraries after size selection. Top: long-size library; Middle: mid-size library; Bottom: short-size library. (**C**) Saturation curve of 349HAP1-1, the bam file was down sampled with Samtools.

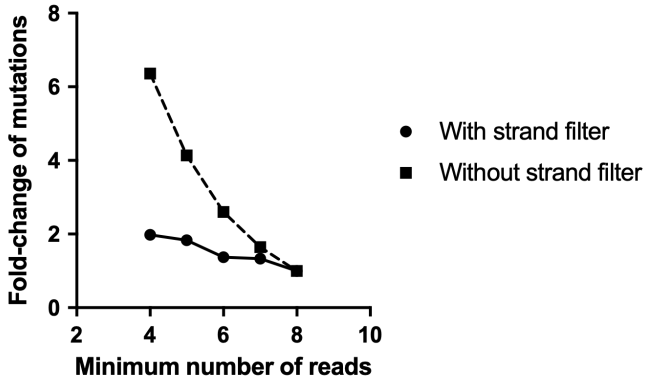

SI Appendix Figure S4

Fold change of detected mutations with regard to the changing of calling threshold in day-5 eHAP single cells. The horizontal axis represents the minimum number of reads required to call a mutation. For calling with the strand filter (solid line), thresholds were set as a4s2, a5s2, a6s3, a7s3 and a8s4. For calling without the strand filter (dashed line), thresholds were set as a4s0, a5s0, a6s0, a7s0 and a8s0. Mutations detected from all single cells were aggregated and normalized by the number of mutations called with at least 8 reads.

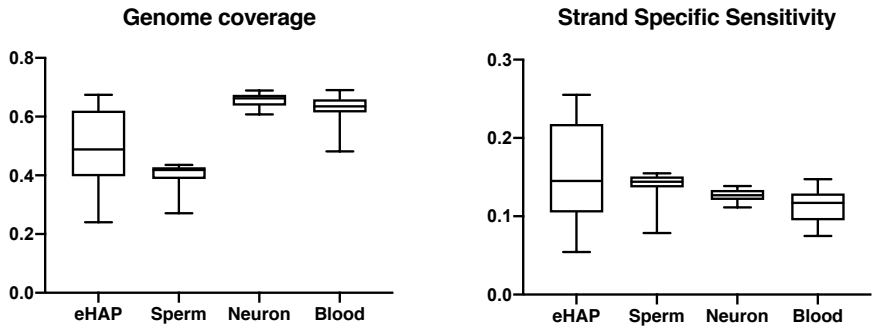

SI Appendix Figure S5

Box and whisker plot of genome coverage and strand specific sensitivity for each category of single cells.

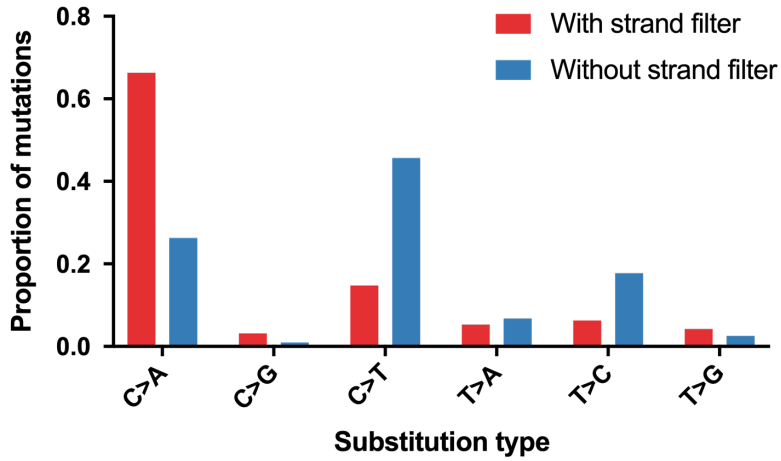

SI Appendix Figure S6

Comparison of mutational spectrum identified with (red) and without (blue) applying the strand filter in day-5 eHAP single cells. Mutations from single cells were pooled to calculate the proportion of each substitution type.

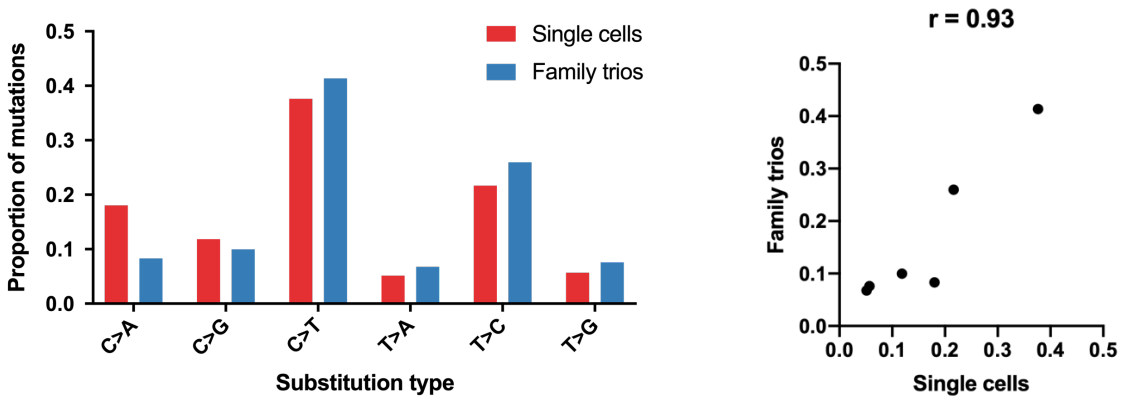

SI Appendix Figure S7

Comparison of mutational spectrum identified from single sperm cells (red) and from family trios (blue) of reference [16]. Mutations were pooled to calculate the proportion of each substitution type. Pearson correlation coefficient was shown above the scatter plot.

SI Appendix Figure S8

Example of DNA damage detected by META-CS viewed in IGV. Reads from two complementary strands are shown in red and blue. Note that the mutated base was only found in one of the two strands.

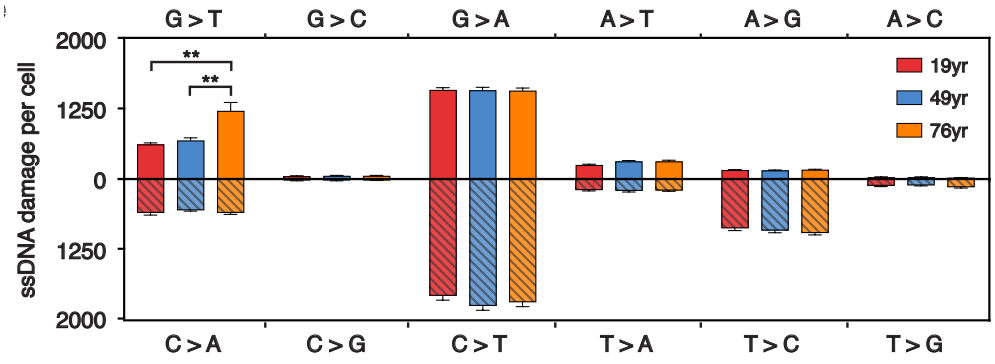

SI Appendix Figure S9

ssDNA damage represented by 16 types of strand specific "mutation" in single neurons from three individuals. Damage of purines are shown at the top half of the panel as solid columns, and damage of pyrimidines are shown at the bottom half of the panel as patterned columns. Data are adjusted by detection efficiency in single cells. Error bars represent standard error. $^{**}P < 0.01$, two-tailed *t*-test.

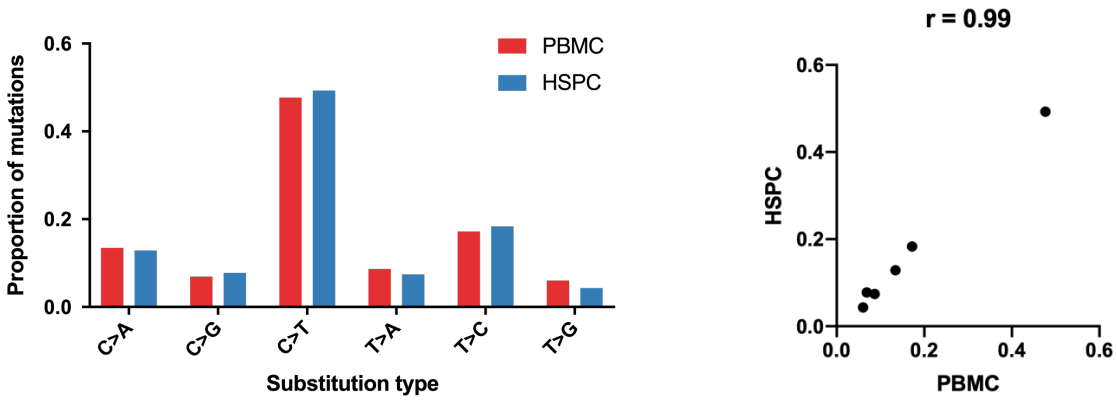

SI Appendix Figure S10

Comparison of mutational spectrum identified from single peripheral blood mononuclear cells (PBMC) (red) and from clonal amplified hematopoietic stem and progenitor cells (HSPC) (blue) of reference [25]. Mutations were pooled to calculate the proportion of each substitution type. Pearson correlation coefficient was shown above the scatter plot.

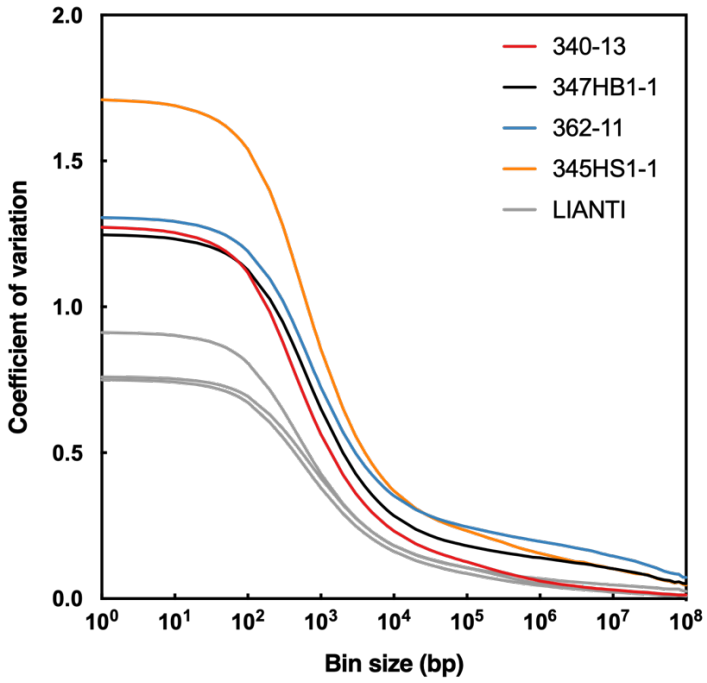

SI Appendix Figure S11

Coefficient of variation for read depths along the genome as a function of bin size. Data of 4 representative cells, 340-13(PBMC), 347HB1-1(PBMC), 362-11(neuron) and 345HS1-1(sperm), are shown together with three single cells amplified by LIANTI. Coefficient of variation of each single cell is calculated in the same way as in reference [2].

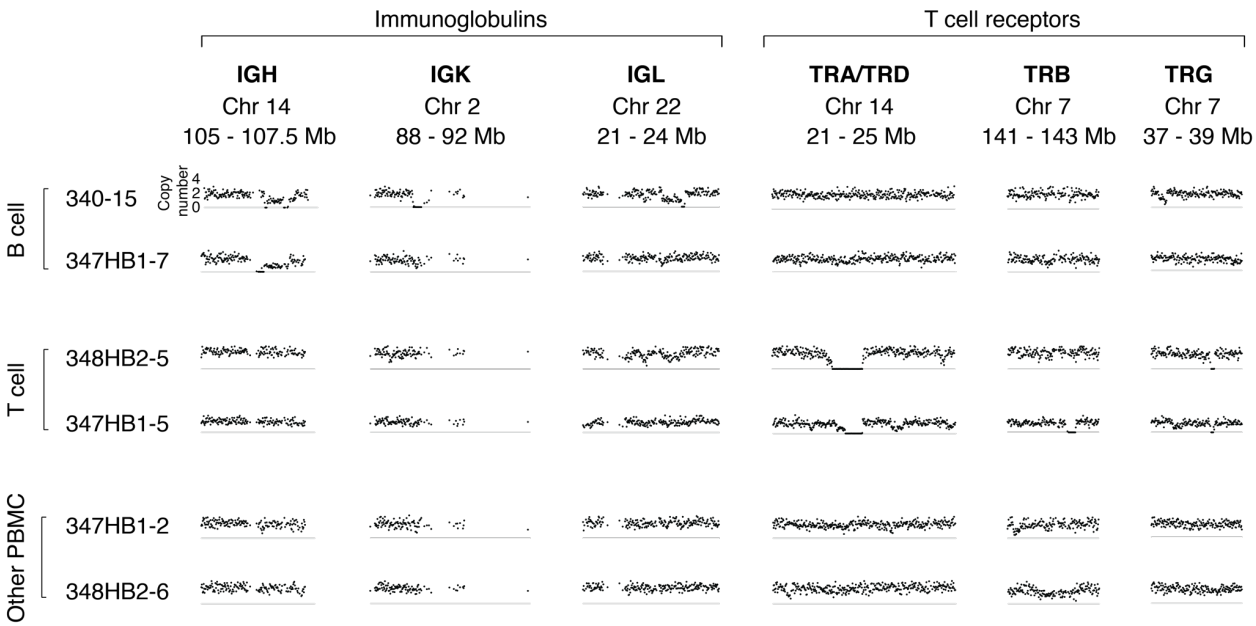

SI Appendix Figure S12

Detection of V(D)J recombination through copy-number changes in representative cells. Each dot represented the normalized average depth of a 10-Kb bin after repeat masking [2].

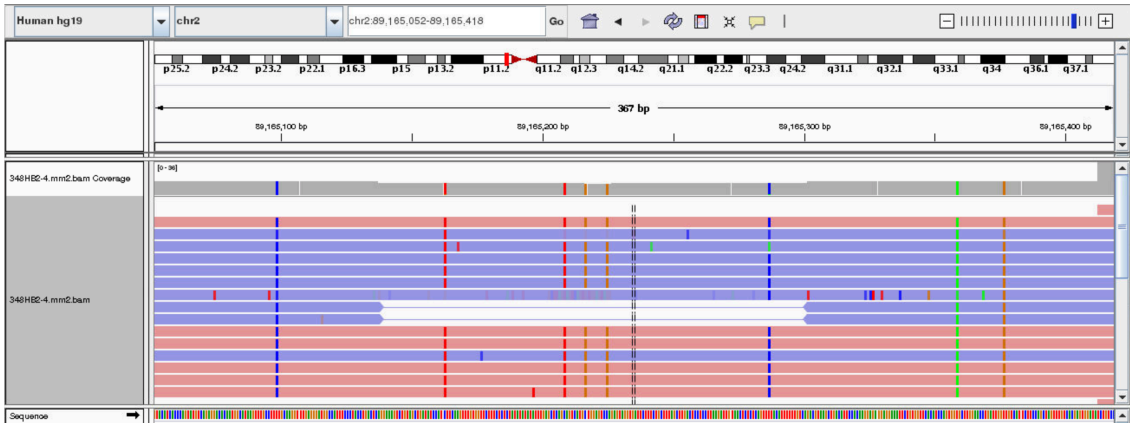

SI Appendix Figure S13

Example of a somatic hypermutation (SHM) region from a representative cell viewed in IGV. Reads from two complementary strands were shown in red and blue. Mutational bases were shown as colored lines. A total of 8 mutations were detected within a region of ~300 bp in the human immunoglobulin kappa locus.

SI Appendix Figure S14

Sequence context of guanine/cytosine mutations (n=16) detected on immunoglobulin gene loci of SHM+ B cells. Sequences near the mutable base (position 0) were extracted from GRCh37 with BEDTools. The logo was generated with WebLogo (version 3.6). D=A/G/T, Y=C/T, and W=A/T.

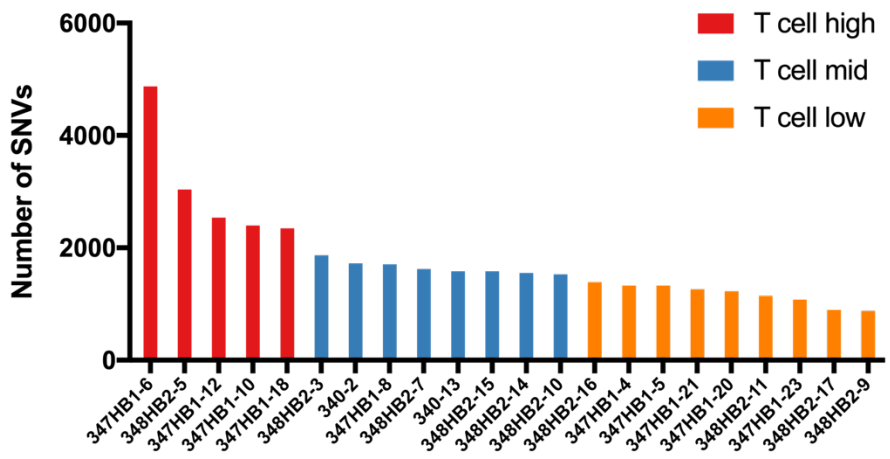

SI Appendix Figure S15

T cells were divided into three subgroups (high, mid and low) based on the number of SNVs identified from each single cell.

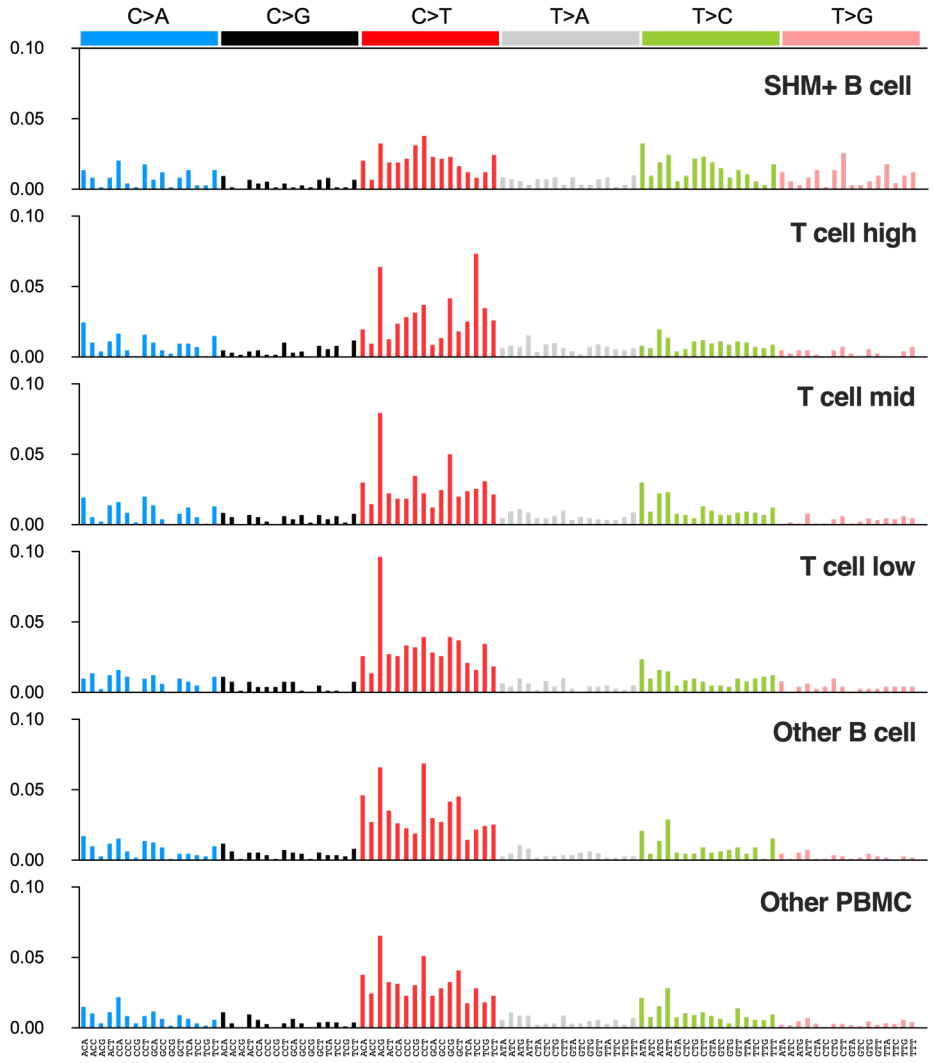

SI Appendix Figure S16

Relative contribution of 96 mutation types for subgroups of PBMCs. Data are represented as the mean contribution of each mutation type from all single cells within the group.

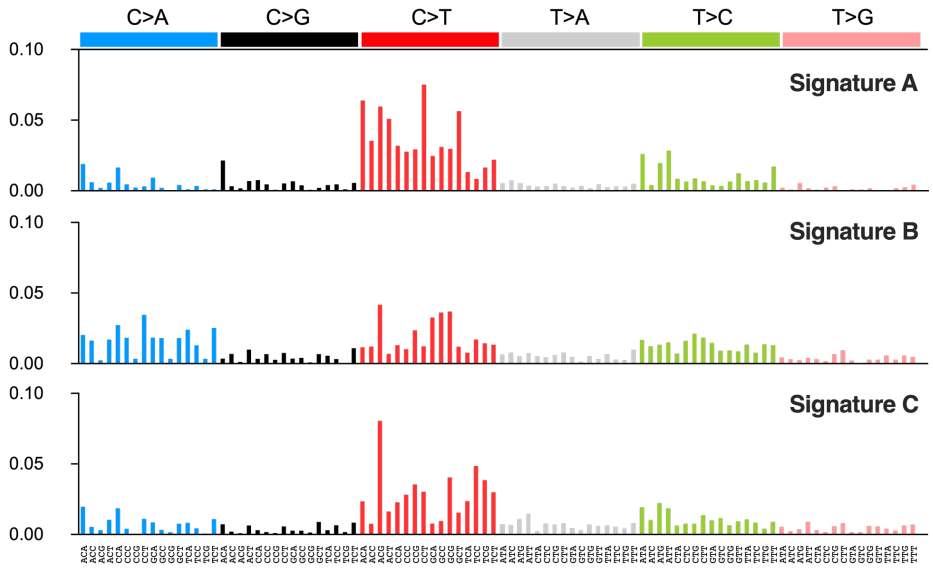

SI Appendix Figure S17

Three mutational signatures in trinucleotide context identified by non-negative matrix factorization.